Research Article

Mohamed S. Hodhod[#], Abdel-Rhman Z. Gaafar*[#], Bandar M. AlMunqedhi, Abdalla Elzein

Green synthesis, characterization, and evaluation of antibacterial activities of cobalt nanoparticles produced by marine fungal species *Periconia prolifica*

https://doi.org/10.1515/chem-2023-0139
received September 6, 2023; accepted September 25, 2023

Abstract: Bio-nanotechnology provided an ecofriendly synthesis route for various metal nanoparticles by utilizing different biological systems, especially microorganisms, which act as an alternative to the physical and chemical methods. Cobalt nanoparticles (CoNPs) were synthesized by *Periconia prolifica* (Anast.) from intertidal decayed wood samples from the mangrove tree *Avicennia marina* (Forsk.) of Tarout Island, located in the Arabian Gulf Sea of Saudi Arabia. CoNPs were characterized by X-ray diffraction, transmission electron microscopy, Fourier-transform infrared spectroscopy, and atomic force microscope. The extract of the culture of *P. prolifica* was used as a bio-reductant agent, during which the culturing process proved to have great potential to be applied on an industrial scale, as it was a time-saving, inexpensive, and adequate amount of biomass being produced at the end of the process. A preliminary antibacterial test against one Gram-positive resistant bacteria (i.e., Methicillin-resistant *Staphylococcus aureus*) and other Gram-negative resistant bacteria was performed using a disk diffusion assay. The antibacterial results witnessed the key role that metal size plays in causing higher activity and also in causing severe damage to the bacterial cells by inactivating its membrane permeability, leading to bacterial cell death.

Keywords: marine fungi, *Periconia prolifica*, CoNPs, characterization, antibacterial activity

1 Introduction

Nanotechnology opened a new frontier for reexploring the properties of metals by manipulating their size, chemical composition, and dimensions to alter their effect [1]. Various methodologies (i.e., chemical and physical routes) are now available to synthesize nanomaterials that can effectively kill drug-resistant bacteria. However, these methods suffer from a few drawbacks due to concerns raised over environmental pollution, since the above-mentioned routes generate massive amounts of hazardous toxic by-products, in addition to high cost and higher reaction conditions (temperature, pH, etc.) [2]. Recently, the development of cost-effective metal nanoparticles (m-NP) based on the principles of green chemistry (i.e., nano-biotechnology) was achieved through the exploitation of biological systems such as plants, algae, fungi, and bacteria [3–5]. Among the biological agents, fungi possessed higher rates of tolerance and metal bioaccumulation abilities, which are crucial characteristics for the synthesis of nanoparticles. Another important benefit of using fungi in the pharmaceutical industry is the ease of scaling up the synthesis process, making the entire process more cost-effective [6]. Thus, there is a demand for the search for new fungal resources and their utilization for the production of nanomaterials.

Marine fungi provide great potential in biotechnological applications [7], as they are a unique ecological group that differs from its terrestrial and freshwater counterparts in

Both authors are considered as first authors.

* **Corresponding author: Abdel-Rhman Z. Gaafar,** Department of Botany and Microbiology, College of Science, King Saud University KSU, P.O. Box 11451, Riyadh, Saudi Arabia, e-mail: agaafar@ksu.edu.sa, tel: +966-540329167
Mohamed S. Hodhod: Faculty of Biotechnology, October University for Modern Sciences & Arts, 6th October City, 12566, Egypt, e-mail: mshodhod@msa.edu.eg
Bandar M. AlMunqedhi: Department of Botany and Microbiology, College of Science, King Saud University KSU, P.O. Box 11451, Riyadh, Saudi Arabia, e-mail: balmunqedhi@ksu.edu.sa
Abdalla Elzein: Institute of Integrative Nature Conservation Research (INF), Department of Integrative Biology and Biodiversity Research (DIBB), University of Natural Resources and Life Sciences (BOKU), Vienna, Austria, e-mail: abdalla.elzein@boku.ac.at
ORCID: Abdel-Rhman Z. Gaafar 0000-0001-6218-9572

both physiological and morphological requirements [8]; they are found exclusively in oceans and seas of the world colonizing a wide variety of decaying plant material ranging from mangroves, drift and intertidal wood, algae, seagrasses, corals, and various marine animals [9]. *Periconia prolifica* has been reported from different substrata in Saudi Arabia, including Jeddah driftwood [10], mangroves wood [11], and from the coast of the Red Sea coast, and seawater and sea foam from the Arabian Gulf coast [12]. The current effort focuses on two important points: (i) the green synthesis of cobalt nanoparticles (CoNPs) utilizing a fungal extract of *P. prolifica*, which will aid in developing nanostructures, minimize light recombined activity, and boost reactive oxygen species activities. (ii) Evaluation of the effect of CoNPs on eradicating *Escherichia coli* and Methicillin-resistant *Staphylococcus aureus* (MRSA) bacterial strains.

2 Materials and methods

2.1 Fungal isolation and bacterial growth conditions

The marine fungal species *P. prolifica* was recorded from intertidal decayed wood samples of the mangrove tree *Avicennia marina* (Forsk.) of Tarout island located at the Arabian Gulf Sea of Saudi Arabia, with coordinates of (26°35′43″N – 50°3′51″E). The isolated fungi were identified based on the morphological characteristics of the fruiting structures (i.e., conidiomata, conidiogenesis, conidiophores, and conidia for anamorphic fungi) [13]. The conidia were mounted in seawater for photography, measurements, and description using the compound microscope (Motic ACCUscope 3002, China) and examined using a scanning electron microscope (SEM) (JOEL, JSM-6380 LA, Tokyo, Japan). The germinated conidia were then transferred to new Petri plates of glucose yeast agar with sterile forceps and incubated at 25°C for 1–2 weeks in the dark [14]. Pure cultures of isolated fungi were preserved in a glycerol solution (10%) at −80°C and deposited at the Department of Botany and Microbiology of Science, King Saud University.

The test organisms included Gram-negative resistant *E. coli* ATCC BAA-196 and Gram-positive MRSA ATCC-33591. Pathogenic bacterial strains were grown for 24 h on Muller-Hinton agar plates, and a cell suspension was prepared in physiological saline (phosphate buffer saline).

2.2 Biosynthesis of CoNPs

For nanoparticle green synthesis, *P. prolifica* was cultivated in 250 Erlenmeyer flasks containing 100 ml of YMG 50% seawater medium. Cultured flasks were incubated in a rotating shaker at 200 rpm for 5 days at 25°C. Cobalt metal in the form of cobalt chloride ($CoCl_2$) was introduced to the supernatant to test extracellular bio-reduction [15]. The biosynthesis of nanoparticles was carried out using 5 mM of the metal salt solution followed by rationally adding supernatant (i.e., 90 ml of metal salt solution + 10 ml of supernatant), where instant development of color occurs (i.e., dark yellow) indicating the bio-reduction of metal salt. The flasks were then placed on a rotating shaker (200 rpm) at 25°C for 72 h in the dark to complete the reduction process (Figure 1).

2.3 Characterization of Co-NPs

2.3.1 Ultraviolet-visible (UV–vis) spectroscopy

CoNP biosynthesis was monitored by measuring 1 ml of $CoCl_2$-treated cell-free filtrate (CFF) at regular intervals using a UV spectrophotometer (UV-1800 Shimadzu Spectrophotometer, Japan).

2.4 X-ray diffraction (XRD)

The average mean size of Co-NPs was determined by XRD spectroscopy (XRD-Ultima IV Rigaku, United States of America) on films of the respective solutions drop-coated onto glass substrates on an XRD machine. The Scherer equation $d = 0.9\lambda/\beta \cos\theta$ was used to estimate the mean size of the nanoparticles produced, where d is the mean diameter of the nanoparticles, λ is the wavelength of the X-ray radiation source, β is the full angular width at half maximum of the XRD peak at the diffraction angle, and θ is the Bragg angle [16].

2.5 Transmission electron microscopy (TEM)

The morphology of the synthesized CoNPs including their shape and size was analyzed and measured using a TEM instrument (JEOL-JEM-1011, Tokyo, Japan). The sample was

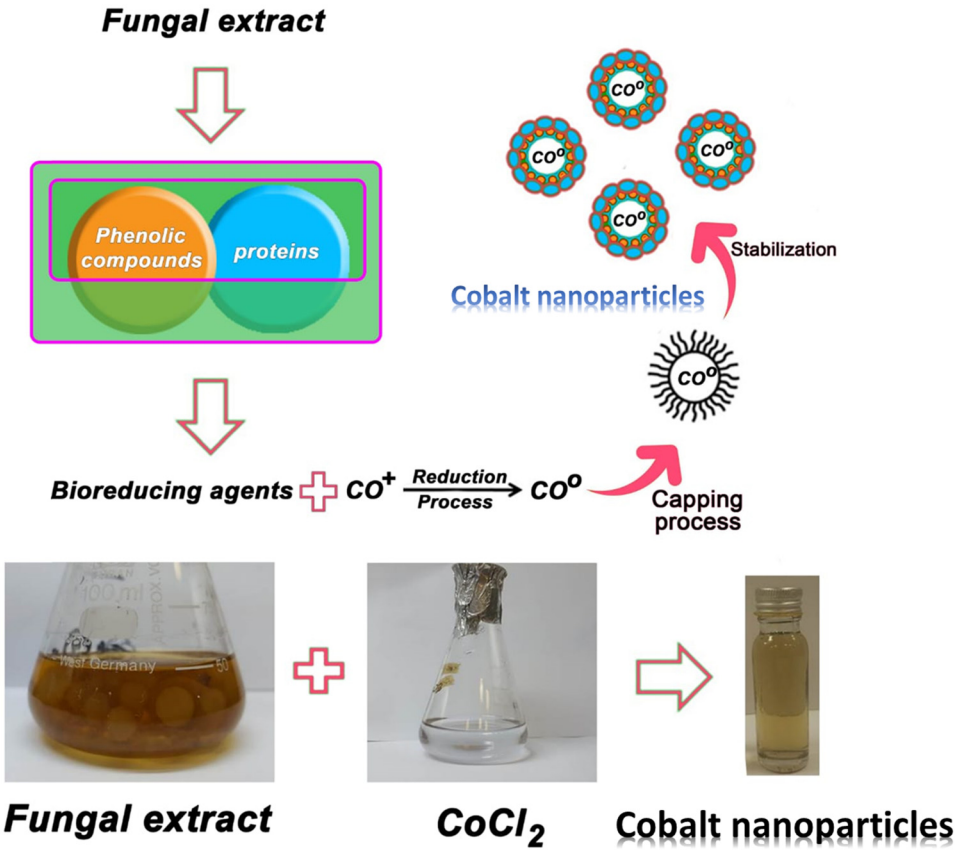

Figure 1: The proposed mechanism of biosynthesis of CoNPs via *P. prolifica* extract.

prepared by drop-coating nanoparticle solutions (100%) onto carbon-coated copper TEM grids. The films on the TEM grids were allowed to stand for 2 min, and the grid was then allowed to dry before measurement.

2.6 Fourier transform infrared (FTIR) spectroscopy

CoNP analysis was performed using FTIR spectroscopy (Perkin-Elmer 1000 FT-IR, USA), and dry powders of the nanoparticles were obtained in the following manner. The biosynthesized nanoparticles were centrifuged at 14,000 rpm for 15 min, after which the pellet was re-dispersed in sterile distilled water to remove any uncoordinated biological molecules. The process of centrifugation and redistribution in sterile distilled water was repeated three times to ensure better separation of free entities from the m-NPs. The purified pellets were then dried, and the powders were subjected to FTIR spectroscopy measurement.

2.7 Antibacterial activity

A preliminary test was carried out against one Gram-positive resistant bacteria (i.e., MRSA) and other Gram-negative resistant bacteria (i.e., *E. coli*) using disk diffusion assay [17]. To determine the effect of the antibacterial potential possessed by the synthesized m-NPs, an atomic force microscope (AFM) was applied to determine the effect of CoNPs on the bacterial cells.

3 Results and discussion

Periconia prolifica has been reported from different geographical locations around the world, including Egypt, Saudi Arabia, Kuwait, Ghana, South Africa, Brazil, Malaysia, Indonesia, Japan, China, Mexico, the USA, and Taiwan; the substrates reported comprised decayed intertidal mangrove wood and seedlings [10,18,19]. *P. prolifica* conidia is characterized by 1-celled (6–13 × 20 µm), ovoid, smooth, and light brown with a reddish tint (Figure 2).

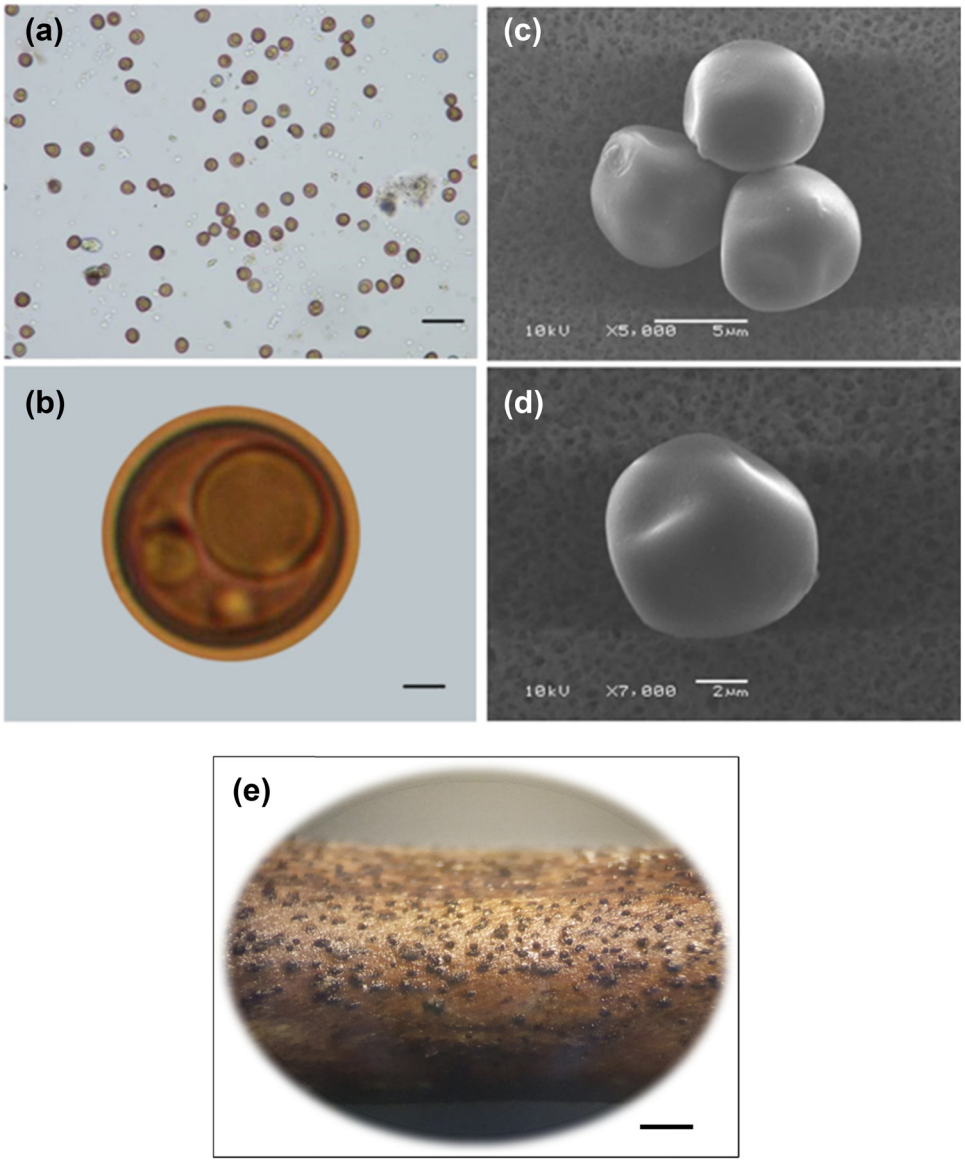

Figure 2: *P. prolifica*. (a) and (b) Bright-field light micrographs (from the holotype mounted in water). (c) and (d) SEM. (c) Group of smooth-walled conidia. (d) Magnified conidia. (e) Dissecting microscope, conidia on the wood surface. Bars: *A* = 30 µm, *C* = 5 µm, *B* and *D* = 2 µm, *E* = 500 µm.

Spectral absorption of CoNP (Figure 3) was produced using CFF of *P. prolifica* (purple curve), and the dark yellow color developed in the solution resulting from the reduction of the metal salt. The blue curve indicates the control group, which has a transparent color in the solution as an indicator of CoNPs. The high optical density of the CoNP solution was recorded at 420 nm, while the control group did not have a peak at 300–800 nm. The UV visible spectroscopy results of CoNPs synthesized by *P. prolifica* showed a very close absorbance of 420 nm, indicating a surface plasmon resonance, which indicates that the synthesized nanoparticle sizes are smaller than 100 nm. The reading absorbance is due to the excitation of electrons in the conductive band around the nanoparticle surface [20]. The change in absorbance reading indicates that the produced nanoparticles are of different shapes and sizes [21].

The CoNp diffraction peaks (Figure 4) corresponded to the characteristic face-centered cubic cobalt lines indexed as (2.389), (2.068), and (1.386) that were observed in these samples at diffraction angles of 37.8°, 43.9°, and 76.8°, respectively. The mean size of the CoNPs estimated by XRD data is 21 nm. The CoNP data obtained perfectly matched the database Joint Committee on Powder Diffraction Standards (JCPDS) database file No. 73-2134 (23).

The TEM results presented in Figure 5 of the *P. prolifica* CoNP appeared to be a pentagonal shape with an average

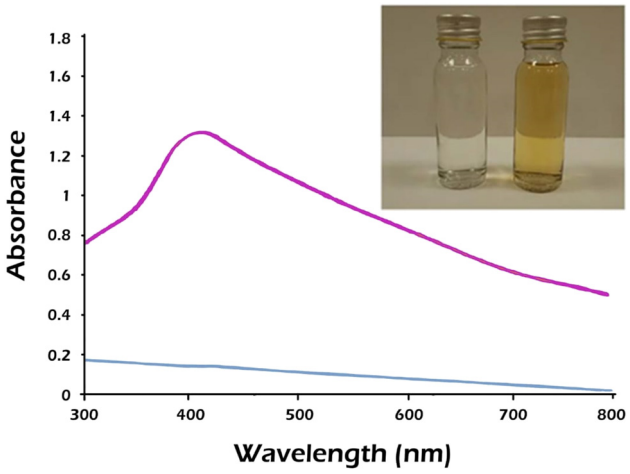

Figure 3: UV–visible spectra of CoNPs synthesized using *P. prolifica* CFF (purple curve), and the control group is represented herein by the blue curve.

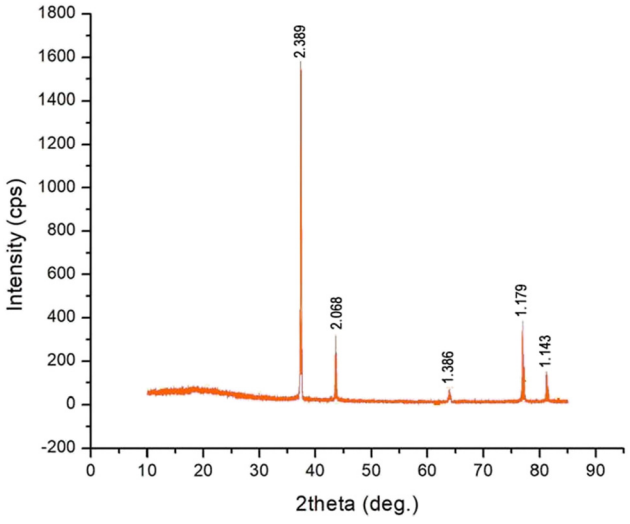

Figure 4: XRD pattern of CoNPs synthesized by *P. prolifica*.

mean size of 21 nm. The results of both XRD and TEM matched perfectly with each other, confirming the characteristics and properties of the produced m-NPs [23,24].

FTIR spectroscopy (Figure 6) was used to determine the chemical functional groups in the cobalt m-NPs and proteins surrounding the synthesized nanoparticles as stabilization agents.

FTIR analysis involved in the formation of CoNPs included the presence of peaks at 3,427 and 3,273 cm^{-1} in *P. prolifica* corresponding to the hydroxyl group of polyphenolic compounds. The bands shown at 2,963, 2,924, and 2,851 cm^{-1} are assigned to –CN stretching vibrations. The presence of peaks at 1,630 and 1,535 cm^{-1} corresponds to the C═O and NH (primary amine) of peptide linkage, respectively. The band for

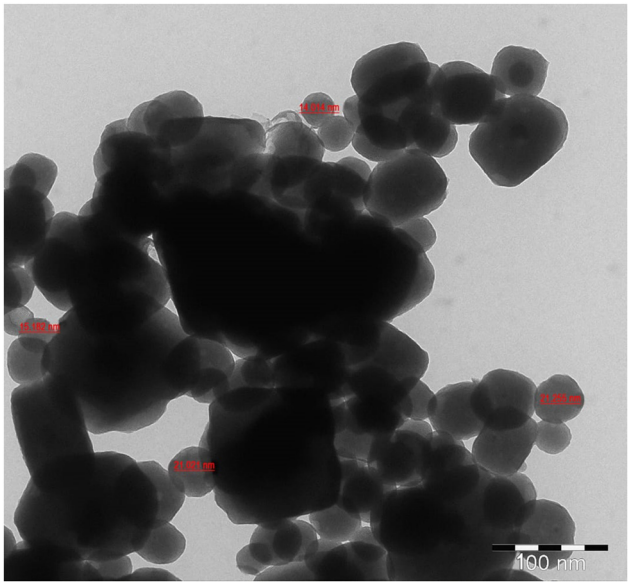

Figure 5: TEM micrograph of CoNPs showing the shape and particle size estimation, where cobalt takes a pentagonal shape with an average mean size of 21 nm.

1,454 and 1,406 cm^{-1} was assigned to the stretching of the aromatic amino group. The peak shown at 1,234 cm^{-1} corresponds to the presence of aromatic rings. FTIR analysis confirmed the presence of proteins surrounding and coating synthesized CoNPs, which act as reducing agents and stabilizing agents during the biosynthesis process [25,26].

The results of the CoNP characterization showed similar observations to many studies. The UV visible spectroscopy results were compatible with many reports. The distinguishing characteristic of CoNPs is to exhibit a surface plasmon absorption band in the range of 350–550 nm [27,28]. The change in absorbance reading indicates that the produced nanoparticles are of different shapes and sizes [21]. The XRD results of the obtained CoNP data were matched perfectly with the JCPDS file of database no. 73–2134 [22], which was also reported in other studies with slightly different angles [29–31]. The TEM results of the CoNPs appeared to be pentagonal in shape with an average mean size of 21 nm. A size similar to that observed in other studies [31,32]. FTIR analysis confirmed the presence of proteins surrounding and coating synthesized CoNPs, which act as reducing agents and stabilizing agents during the biosynthesis process [27,33].

The preliminary antibacterial activity test (Figure 7, Table 1) against Gram-negative resistant *E. coli* and Gram-positive MRSA showed an inhibition zone of 13 and 15 mm, respectively.

The CoNPs were shown to have supreme antibacterial activity (Figure 8). As Co+ small particles resulted in increased surface area, which led to better surface contact with bacteria

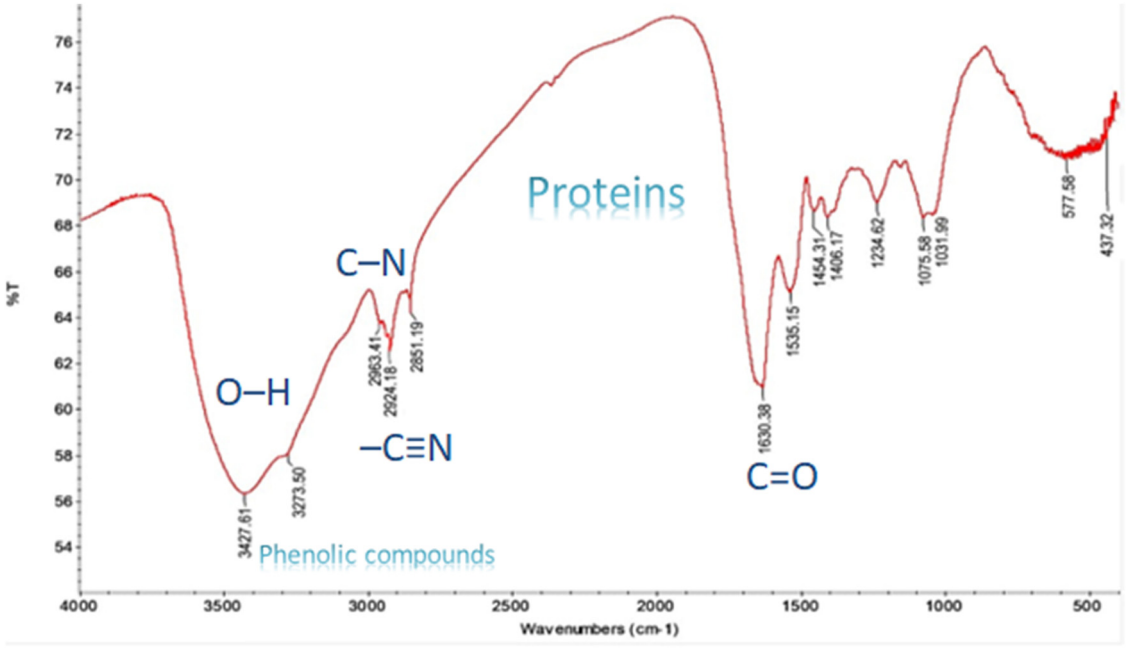

Figure 6: FTIR of the synthesized CoNPs.

and hence better bactericidal effect [34–36]. AFM images at time zero showed that Co+ ions are believed to create an electrostatic bond to the bacterial outer surface, where once that contact is made, the bacterial cells are oxidized and damaged instantly. This is due to the release of CoNP ions that react directly with the thiol (–SH) group of proteins located at the bacterial cell and protrude through the cell membrane. Therefore, inactivating membrane permeability leads to bacterial cell death [37]. Antibacterial results witnessed the key role played by metal size in causing higher activity and in targeting behavior mechanisms. CoNP activity has been reported in many studies; mechanisms of action include its surface binding to bacterial membranes, therefore increasing the generation time by decreasing cell mobility [38]. Other mechanisms involving the stimulation of reactive oxygen formation, such as super-oxide ($-O_2$) and hydrogen

Table 1: Minimum inhibitory concentration (MIC) of CoNPs against Gram-positive and negative bacterial species

Bacterial species	Gram	MIC (µg/ml)	Inhibition zone
E. coli	−ve	4 ± 0	13.4 ± 1.34
MRSA	+ve	2 ± 0	15.2 ± 1.3

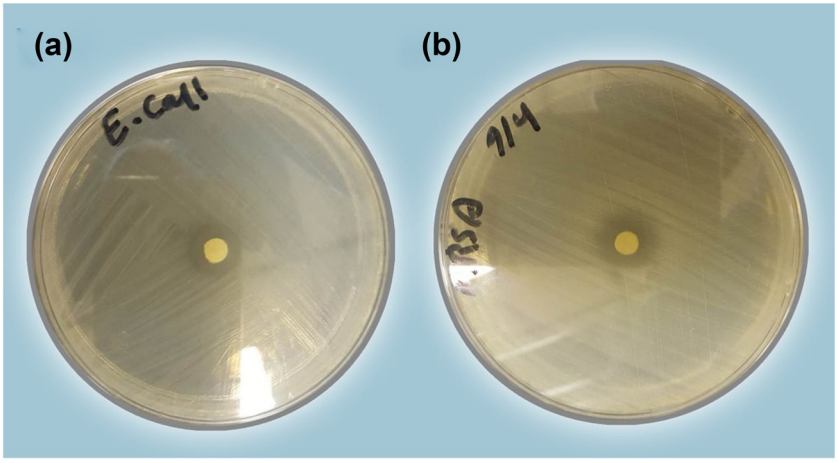

Figure 7: Agar disc diffusion method using CoNPs against (a) *E. coli* and (b) MRSA.

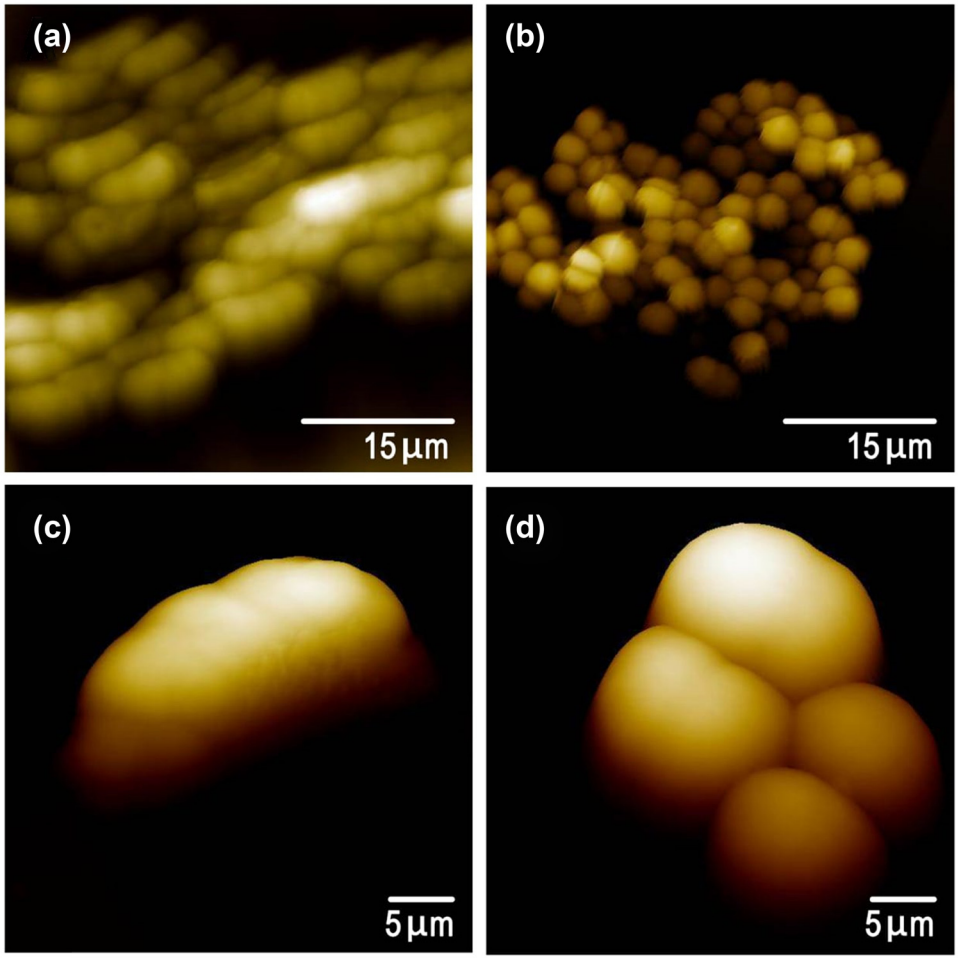

Figure 8: (a)–(d) AFM using CoNPs against *E. coli* and MRSA at time = 0. (a) and (b) Aggregates of bacterial cells taken at a lower magnification of *E. coli* and MRSA respectively, (c) and (d) Magnified bacterial cells of *E. coli* and MRSA, respectively.

peroxide (H_2O_2), result in more damage to the cell through essential proteins, genomic and plasmid DNA degradation [39–43].

4 Conclusion

The economic synthesis of stable pentagonal CoNPs via new biological resources such as marine fungi for use as antibacterial agents was very promising. The extract of the culture of *P. prolifica* was used as a bio-reductant agent, during which the culturing process proved to have great potential to be applied on an industrial scale, as it was a timesaving, cheap, and adequate amount of biomass being produced at the end of the process. The presence of proteins was detected through FTIR, which was found to coat the synthesized CoNPs, which act as reducing and stabilizing agents in the reduction process. Although the produced nanoparticles were of moderate size, they revealed elevated antibacterial activity. AFM imaging was of great aid in showing the mechanism of action on the bacterial cell surfaces, which was revealed by their swelling due to the inactivation of the cell membrane permeability, resulting in eventual bacterial death. Further in-depth studies must be conducted using other marine fungal species, and other biotechnological applications could be performed including anticancer, antioxidant, and insecticidal activity.

Acknowledgments: The authors appreciate the Researchers Supporting Project number RSPD2023R686, King Saud University, Riyadh, Saudi Arabia.

Funding information: The Researchers Supporting Project number RSPD2023R686, King Saud University, Riyadh, Saudi Arabia.

Author contributions: All authors contributed to the preparation of the manuscript and the discussion. M.S.H. and

A.-R.Z.G. gave the idea, supervised the experiments, and reviewed the final draft of the manuscript. A-R.Z.G., M.S.H., and B.M.A. performed the experiments, analyzed the data, and wrote the first draft. A.Z. helped in data analysis. M.S.H. helped in field data collection.

Conflict of interest: On behalf of all authors, the corresponding author states that there is no conflict of interest.

Data availability statement: All data generated or analyzed during this study are included in this published article.

References

[1] Levy SB, Marshall B. Antibacterial resistance worldwide: causes, challenges and responses. Nat Med. 2004;10(12s):S122.

[2] Soufi A, Hajjaoui H, Elmoubarki R, Abdennouri M, Qourzal S, Barka N. Spinel ferrites nanoparticles: synthesis methods and application in heterogeneous Fenton oxidation of organic pollutants–a review. Appl Surf Sci Adv. 2021;6:100145.

[3] Nachiyar V, Sunkar S, Prakash P. Biological synthesis of gold nanoparticles using endophytic fungi. Der Pharma Chem. 2015;7(11):31–8.

[4] Ottoni CA, Simões MF, Fernandes S, Dos Santos JG, Da Silva ES, de Souza RFB, et al. Screening of filamentous fungi for antimicrobial silver nanoparticles synthesis. AMB Express. 2017;7(1):31.

[5] Shende S, Ingle AP, Gade A, Rai M. Green synthesis of copper nanoparticles by Citrus medica Linn.(Idilimbu) juice and its antimicrobial activity. World J Microbiol Biotechnol. 2015;31(6):865–73.

[6] Saxena J, Sharma PK, Sharma MM, Singh A. Process optimization for green synthesis of silver nanoparticles by Sclerotinia sclerotiorum MTCC 8785 and evaluation of its antibacterial properties. SpringerPlus. 2016;5(1):1–10.

[7] Hodhod MSE-D, Gaafar A-RZ, Alshameri A, Qahtan AA, Noor A, Abdel-Wahab M. Molecular characterization and bioactive potential of newly identified strains of the extremophilic black yeast Hortaea werneckii isolated from Red Sea mangrove. Biotechnol Biotechnol Equip. 2020;34(1):1288–98.

[8] Jones EG. Marine fungi: some factors influencing biodiversity. Fung Divers. 2000;4:53–73.

[9] Jones EG, Pang K-L. Tropical aquatic fungi. Biodivers Conserv. 2012;21:2403–23.

[10] Aleem A. A contribution to the study of seagrasses along the Red Sea coast of Saudi Arabia. Aquat Botany. 1979;7:71–8.

[11] Hodhod MS. Molecular Systematics of Marine Fungi Isolated from Yanbu Mangroves in the Kingdom of Saudi Arabia. Saudi Arabia: King Saud University; 2013.

[12] Bokhary H, Moslem M, Parvez S. Marine fungi of the Arabian Gulf coast of Saudi Arabia. Microbiologica (Bologna). 1992;15(3):281–9.

[13] Jones EG, Suetrong S, Sakayaroj J, Bahkali AH, Abdel-Wahab MA, Boekhout T, et al. Classification of marine ascomycota, basidiomycota, blastocladiomycota and chytridiomycota. Fungal Diversity. 2015;73:1–72.

[14] Abdel-Wahab MA, Bahkali AH, Jones EG, Elgorban AM, Abdel-Aziz FA, Hodhod MS, et al. Two new species of Kallichroma (Bionectriaceae, Hypocreales) from Saudi Arabian mangroves. Phytotaxa. 2016;260(1):66–74.

[15] Das VL, Thomas R, Varghese RT, Soniya E, Mathew J, Radhakrishnan E. Extracellular synthesis of silver nanoparticles by the Bacillus strain CS 11 isolated from industrialized area. 3 Biotech. 2014;4(2):121–6.

[16] Cullity BD. Elements of X-ray diffraction. Mass: Addison Wesley; 1978.

[17] Balouiri M, Sadiki M, Ibnsouda SK. Methods for in vitro evaluating antimicrobial activity: A review. J Pharm Anal. 2016;6(2):71–9.

[18] Abdel-Wahab MA. Diversity of marine fungi from Egyptian Red Sea mangroves. Bot Mar. 2005;48(1):348–55.

[19] Pang K-L, Jheng J-S, Jones EG. Marine mangrove fungi of Taiwan. Chilung: National Taiwan Ocean University; 2011. p. 1–131.

[20] Fultz B, Howe JM. Transmission electron microscopy and diffractometry of materials. Germany: Springer Berlin Heidelberg; 2012.

[21] Desai R, Mankad V, Gupta SK, Jha PK. Size distribution of silver nanoparticles: UV-visible spectroscopic assessment. Nanosci Nanotechnol Lett. 2012;4(1):30–4.

[22] Ranganatha S, Munichandraiah N. Synthesis and performance evaluation of novel cobalt hydroxychlorides for electrochemical supercapacitors. J Solid State Electrochem. 2017;21(4):939–46.

[23] Chicea D, Indrea E, Cretu C. Assesing Fe3O4 nanoparticle size by DLS, XRD and AFM. J Optoelectron Adv Mater. 2012;14(5):460.

[24] Hu C, Zhang Z, Liu H, Gao P, Wang ZL. Direct synthesis and structure characterization of ultrafine CeO2 nanoparticles. Nanotechnology. 2006;17(24):5983.

[25] Daima HK, Selvakannan P, Shukla R, Bhargava SK, Bansal V. Fine-tuning the antimicrobial profile of biocompatible gold nanoparticles by sequential surface functionalization using polyoxometalates and lysine. PLoS one. 2013;8(10):e79676.

[26] Saxena J, Sharma PK, Sharma MM, Singh A. Process optimization for green synthesis of silver nanoparticles by Sclerotinia sclerotiorum MTCC 8785 and evaluation of its antibacterial properties. SpringerPlus. 2016;5(1):861.

[27] Bibi I, Nazar N, Iqbal M, Kamal S, Nawaz H, Nouren S, et al. Green and eco-friendly synthesis of cobalt-oxide nanoparticle: Characterization and photo-catalytic activity. Adv Powder Technol. 2017;28(9):2035–43.

[28] Jain PK, Lee KS, El-Sayed IH, El-Sayed MA. Calculated absorption and scattering properties of gold nanoparticles of different size, shape, and composition: applications in biological imaging and biomedicine. J Phys Chem B. 2006;110(14):7238–48.

[29] Dhas NA, Raj CP, Gedanken A. Synthesis, characterization, and properties of metallic copper nanoparticles. Chem Mater. 1998;10(5):1446–52.

[30] Nazeruddin G, Prasad N, Prasad S, Garadkar K, Nayak AK. In-vitro bio-fabrication of silver nanoparticle using Adhathoda vasica leaf extract and its anti-microbial activity. Phys E: Low-dimensional Syst Nanostruct. 2014;61:56–61.

[31] Salavati-Niasari M, Khansari A, Davar F. Synthesis and characterization of cobalt oxide nanoparticles by thermal treatment process. Inorganica Chim Acta. 2009;362(14):4937–42.

[32] Nethravathi C, Sen S, Ravishankar N, Rajamathi M, Pietzonka C, Harbrecht B. Ferrimagnetic nanogranular Co3O4 through solvothermal decomposition of colloidally dispersed monolayers of α-cobalt hydroxide. J Phys Chem B. 2005;109(23):11468–72.

[33] Fischer UA, Carle R, Kammerer DR. Identification and quantification of phenolic compounds from pomegranate (Punica granatum L.) peel, mesocarp, aril and differently produced juices by HPLC-DAD–ESI/MSn. Food Chem. 2011;127(2):807–21.
[34] Cho K-H, Park J-E, Osaka T, Park S-G. The study of antimicrobial activity and preservative effects of nanosilver ingredient. Electrochim Acta. 2005;51(5):956–60.
[35] Panyala NR, Peña-Méndez EM, Havel J. Silver or silver nanoparticles: a hazardous threat to the environment and human health? J Appl Biomed (De Gruyter Open). 2008;6(3):117–29.
[36] Prabhu S, Poulose EK. Silver nanoparticles: mechanism of antimicrobial action, synthesis, medical applications, and toxicity effects. Int Nano Lett. 2012;2(1):32.
[37] Zhang H, Chen G. Potent antibacterial activities of Ag/TiO2 nanocomposite powders synthesized by a one-pot sol− gel method. Environ Sci Technol. 2009;43(8):2905–10.
[38] Vidya R, Venkatesan K. Preparation and characterization of zinc ferrite (ZnFe2O4) nanoparticles using self-propagated combustion route and evaluation of antimicrobial activity. Res J Pharm Biol Chem Sci. 2015;6(1):537–42.
[39] Chatterjee AK, Chakraborty R, Basu T. Mechanism of antibacterial activity of copper nanoparticles. Nanotechnology. 2014;25(13):135101.
[40] Dupont CL, Grass G, Rensing C. Copper toxicity and the origin of bacterial resistance—new insights and applications. Metallomics. 2011;3(11):1109–18.
[41] Hashim M, Shirsath SE, Meena S, Kotnala R, Parveen A, Roy AS, et al. Investigation of structural, dielectric, magnetic and antibacterial activity of Cu–Cd–Ni–FeO4 nanoparticles. J Magn Magn Mater. 2013;341:148–57.
[42] Sawai J. Quantitative evaluation of antibacterial activities of metallic oxide powders (ZnO, MgO and CaO) by conductimetric assay. J Microbiol Methods. 2003;54(2):177–82.
[43] Xavier S, Cleetus H, Nimila P, Thankachan S, Sebastian R, Mohammed E. Structural and antibacterial properties of silver substituted cobalt ferrite nanoparticles. Res J Pharm Biol Chem Sci. 2014;5(5):364–71.